

# Cubic nonlinear stiffness and quadratic nonlinear piezoelectrical coupling on the dynamic behaviour of an aeroelastic energy harvesting system

Ana Carolina Godoy Amaral<sup>1</sup>, Marcos Silveira<sup>1</sup>

<sup>1</sup>*São Paulo State University (UNESP), School of Engineering  
Av. Eng. Luiz Edmundo C. Coube 14-01, Vargem Limpa, 17033-360, São Paulo/Bauru, Brazil  
ana.carolina@unesp.br, marcos.silveira@unesp.br*

**Abstract.** Nonlinear aspects of energy harvesting have been extensively investigated in the last 10 years for two main reasons: improve the accuracy of the mathematical models of systems that inherently present nonlinear behaviour, and to intentionally introduce nonlinear behaviour to the system in order to improve the harvesting performance. In this paper, we show the contributions of cubic nonlinear stiffness and quadratic nonlinear piezoelectrical coupling on the dynamic behaviour of an aeroelastic energy harvesting system. To analyse each case analytically the method of multiple scales is used. The application of nonlinearity can make systems difficult to solve. Multiple scales is an analytical method to provide an approximate expression of the response of a system. This method work for small periodic finite movements in the vicinity of a equilibrium. One of the advantages of this method is that it allows solving equations in the presence of damping and nonlinearity. Numerically, the response is calculated using a 4<sup>th</sup> order Runge-Kutta method. The amplitude related to plunge, pitch and voltage degrees of freedom as function of the wind speed is analysed for different values of cubic and quadratic nonlinearity. The results indicate that amplitude decreases when cubic nonlinear stiffness and quadratic nonlinear piezoelectrical coupling increase. It is important to observe that the results show good agreement in the LCO amplitudes only near the bifurcation.

**Keywords:** Nonlinear, Energy Harvesting, Flutter, Multiple Scales

## 1 Introduction

Energy harvesting is a technology that has been explored by researchers as an alternative to nonrenewable energy resources in recent years [1], because it is a promising technology to produce sustainable energy sources, replacing fossil fuel. There are many ways to harvest energy: electromagnetic, piezoelectric, thermoelectric, pyroelectric, photovoltaic and solar heat collector [2]. Energy harvesters are designed to extract energy from ambient mechanical vibration and transfer it to electrical devices [3]. Energy harvesting sources include mechanical vibrational, RF, thermal gradient. There are also many types of energy transducers and techniques for energy storage and distribution. It is important to extract the maximum output power to make this technology more viable. One way to maximize energy harvesting power output is to choose the right type of piezoelectric and the right combination of parameters [4]. But harvester performance is still an issue. The study of [5] discusses the work of a piezoelectric harvester, in which efficiency is mainly related to the electromechanical coupling effect, damping effect, excitation frequency and electric charge.

One of the many fields of study in which energy harvesting can be applied is in aeronautics. It has many applications, such as generating low power electricity in various applications, ranging from aircraft and helicopters to civil structures in high wind areas [6]. Aeroelasticity is a science that studies the behaviour and mechanical properties of an elastic section or structure in interaction with air [7]. Flutter is a very important topic in aeroelasticity, the flutter phenomenon occurs when an aircraft component presents a divergent oscillatory self-sustained behaviour at a certain speed. It is an undesirable phenomenon in aircraft, as it can cause structural damage due to aeroelastic instability [8]. But this oscillatory movement is an interesting source of research and study for energy extraction. Besides that, one benefit of using energy harvesting in an aeroelastic system is that it increases the flutter speed, which can be an interesting topic for aeronautics. Another benefit of energy harvesting is extracting electrical energy from vibrating vibrations and directing it to the aircraft's electronic devices.

An important question is how to improve this technology so that it can collect as much energy as possible. Nonlinear elements were studied as a way to maximize power output in the typical aeroelastic section and suppress flutter velocity. Nonlinear stiffness components were investigated on extracted energy and nonlinear aeroelastic

behaviour [9]. The work of Triplett and Quinn [10] compares the use of nonlinear stiffness and nonlinear electromechanical coupling with the typical section with linear stiffness and linear electromechanical coupling, quantifying vibration speed, mechanical and electrical power. It is possible to see that the addition of nonlinear elements changes the system performance, so that the nonlinear electromechanical coupling can increase the system's output power, which allows extracting more energy. Sousa et al. [11] employs an inductor synchronized tap-changer damping (SSDI) technique, capable of dealing with the nonlinear characteristics of the electrical domain of the problem and the use of shape memory alloys (SMA) as an alternative to conventional actuators. The nonlinearity applied to the system, by the SMA and SSDI together, results in a better aeroelastic behaviour, for a speed range 25 % greater than in a linear system.

The application of nonlinearity can make systems difficult to solve. Multiple scales is an analytical method to provide an approximate expression of the response of a system. These methods work for small periodic finite movements in the vicinity of a center [12]. One of the advantages of this method is that it allows solving equations in the presence of damping and nonlinearity. The response of nonlinear dynamics of harvesters are studied using the multiple scale method [13, 14]. The study of [15] applies the method of multiple scales to an aeroelastic system to derive the normal form of the Hopf bifurcation near the flutter onset. The nonlinear control reduces the LCO amplitude.

## 2 Mathematical model

In this section, the model and the dynamical equations of the aeroelastic typical section are described. Also, the mathematical model for aerodynamic loads is presented. Figure 1 shows the model of the aeroelastic typical section of a system with three degrees of freedom: two mechanical degrees of freedom, plunge ( $h$ ) and pitch ( $\alpha$ ), and one electrical degree of freedom, voltage ( $v$ ). The piezoelectric coupling is associated to plunge.

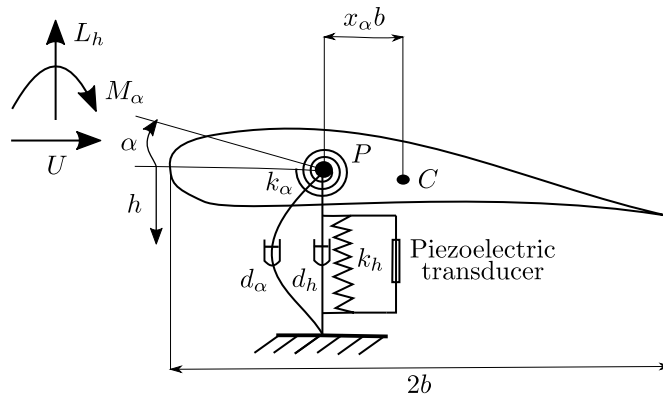


Figure 1. Aeroelastic section.

The dynamical equations, based on [16], of the system presented in fig. 1, applying the nonlinear stiffness of the cubic type associated to plunge movement and nonlinear electromechanical coupling, in dimensionless form, are given by:

$$\begin{aligned} \beta h'' + x_\alpha \alpha'' + \zeta_h h' + h + \delta h^3 - \kappa(K|h'| + 1)v &= -L_h \\ x_\alpha h'' + r_\alpha^2 \alpha'' + \zeta_\alpha \alpha' + \gamma^2 r_\alpha^2 \alpha &= M_\alpha \\ \eta v' + \frac{v}{\lambda} + \kappa(K|h'| + 1)h' &= 0 \end{aligned} \quad (1)$$

in which  $h$  and  $\alpha$  are the dimensionless plunge and pitch displacements,  $\beta$  is the dimensionless mass ratio,  $\zeta_h$  and  $\zeta_\alpha$  are the dimensionless plunge and pitch damping ratios,  $x_\alpha$  is the dimensionless chord-wise offset of the elastic axis from the centroid,  $r_\alpha$  is the dimensionless radius of gyration,  $\gamma$  is the dimensionless frequency ratio,  $M_\alpha$  is the dimensionless aerodynamic moment,  $L_h$  is the dimensionless aerodynamic lift,  $\kappa$  is the dimensionless electromechanical coupling,  $\lambda$  is the dimensionless load resistance,  $v$  is the dimensionless electrical voltage,  $\eta$  is the dimensionless equivalent capacitance,  $\delta$  is the dimensionless nonlinear stiffness coefficient,  $K$  is the dimensionless nonlinear electromechanical coupling coefficient, and  $'$  denotes differentiation over dimensionless time ( $\tau$ ).

The dimensionless terms follows the definitions used by Marqui Jr and Erturk [16], and are reproduced as follows:

$$\begin{aligned}
 h &= \frac{\bar{h}}{b} & \beta &= \frac{m + m_e}{m} & \zeta_h &= \frac{d_h}{m\omega_h} & \zeta_\alpha &= \frac{d_\alpha}{mb^2\omega_h} & r_\alpha &= \frac{\bar{r}_\alpha}{b} \\
 \gamma &= \frac{\omega_\alpha}{\omega_h} & v &= \frac{\bar{v}}{v^*} & \kappa &= \frac{\theta v^*}{cmb\omega_h^2} & \eta &= \frac{C_p v^{*2}}{mb^2c\omega_h^2} & \lambda &= \frac{R_t mb^2 c \omega_h^3}{v^{*2}} \\
 L_h &= \frac{L}{mb\omega_h^2} & M_\alpha &= \frac{M}{mb^2\omega_h^2} & U &= \frac{\bar{U}}{\omega_h b} & \tau &= \omega_h t
 \end{aligned} \tag{2}$$

in which  $m$  is the typical section mass,  $m_e$  is the attachment mass,  $bx_\alpha$  is the offset from the elastic axis to the centroid,  $\bar{h}$  is the plunge displacement,  $d_\alpha$  and  $d_h$  are the plunge and pitch damping coefficients,  $\bar{r}_\alpha$  radius of gyration,  $c$  is the span length,  $\omega_h$  and  $\omega_\alpha$  are the uncoupled plunge and pitch natural frequencies,  $\bar{v}$  is the electrical voltage,  $v^* = 1V$  is the reference voltage for normalisation,  $R_t$  is the load resistance,  $C_p$  is the piezoelectrical equivalent capacitance,  $\theta$  is the piezoelectrical coupling,  $L$  is the aerodynamic lift,  $M$  is the aerodynamic moment,  $\bar{U}$  is the wind speed, and  $t$  is the time.

The model for aerodynamical loads, lift ( $L_h$ ) and moment ( $M_\alpha$ ), is used as presented by Dowell et al. [17] for quasi-steady incompressible flow, and reproduced here:

$$L = \rho \frac{U^2}{2} S \frac{\partial C_L}{\partial \alpha} \left[ \alpha + \frac{\dot{h}}{U} \right] \qquad M = \rho \frac{U^2}{2} S e \frac{\partial C_L}{\partial \alpha} \left[ \alpha + \frac{\dot{h}}{U} \right] \tag{3}$$

in which  $\rho$  is the air density,  $x_f$  is the distance from the leading edge to the neutral line, and  $e = \frac{x_f}{c^{-1/4}}$ . Note that eq. (3) is not in dimensionless form. To include this in eq. (1) one must use the dimensionless forms  $L_h$  and  $M_\alpha$ , given by eq. (2).

## 2.1 Multiple scales analysis

Following the method of multiple scales as described in [12, 15], eq. (1) is put in the form:

$$\dot{Y} = F(Y, U) \tag{4}$$

To present Hopf bifurcation when  $U = U_f$ , a small dimensionless parameter  $\epsilon$  is introduced. Wind speed is expanded as follows:  $U = U_f + \epsilon^2 \sigma_U U_f$ . A third-order solution is sought in the form:

$$Y(t, \sigma_U) = \epsilon Y_1(T_0, T_2), \epsilon^2 Y_2(T_0, T_2), \epsilon^3 Y_3(T_0, T_2) \tag{5}$$

The derivative time is written as follows:

$$\frac{d}{dt} = D_0 + \epsilon^2 D_2 + \epsilon^3 D_3 \tag{6}$$

Replacing eq.(5) and eq.(6) in eq.(4), and separating equations according to the powers of  $\epsilon$  results in:

$$D_0 Y_1 - A(U_f) Y_1 = 0 \tag{7}$$

$$D_0 Y_2 - A(U_f) Y_2 = Q(Y_1, Y_1) \tag{8}$$

$$D_0 Y_3 - A(U_f) Y_3 = -D_2 Y_1 + \sigma_U B Y_1 + 2Q(Y_1, Y_2) + C(Y_1, Y_1, Y_1) \tag{9}$$

in which  $Q$  is the quadratic nonlinear vector  $C$  is the cubic nonlinear vector, and  $B$  is the matrix that contains the coefficients of  $\sigma_U$ :

$$B = \begin{bmatrix} 0 & 0 & 0 & 0 & 0 \\ 0 & 0 & 0 & 0 & 0 \\ 0 & \frac{4\pi U_f^2 \rho \sigma x_\alpha^2 + 4\pi U_f^2 r_\alpha^2 \rho \sigma}{m \omega_h^2 x_\alpha^2 - \beta m \omega_h^2 r_\alpha^2} & \frac{2\pi U_f \rho \sigma x_\alpha^2 + 2\pi U_f r_\alpha^2 \rho \sigma}{m \omega_h^2 x_\alpha^2 - \beta m \omega_h^2 r_\alpha^2} & 0 & 0 \\ 0 & -\frac{4\pi U_f^2 \rho \sigma \beta + 4\pi U_f^2 x_\alpha \rho \sigma}{m \omega_h^2 x_\alpha^2 - \beta m \omega_h^2 r_\alpha^2} & -\frac{2\pi U_f \rho \sigma \beta + 2\pi U_f x_\alpha \rho \sigma}{m \omega_h^2 x_\alpha^2 - \beta m \omega_h^2 r_\alpha^2} & 0 & 0 \\ 0 & 0 & 0 & 0 & 0 \end{bmatrix} \quad (10)$$

The eigenvectors of 10 are also required in the method. The right eigenvector is represented by  $p$ , and the left eigenvector is represented by  $q$  which is normalized as:

$$q = \frac{q}{|q^T p|} \quad (11)$$

System response for the multiple scale method is given by:

$$a = \sqrt{\frac{-4\beta}{\Lambda_a}} \quad (12)$$

in which the parameters  $\Lambda_a$  and  $\beta$  are given by:

$$\Lambda_a = 4q^T Q(p, \zeta_0) + 2q^T Q(\bar{p}, \zeta_2) + 3q^T C(p, p, \bar{p}) \quad (13)$$

$$\beta = q^T \sigma_U B p \quad (14)$$

The values of  $\zeta_0$  e  $\zeta_2$  can be calculated through the equations:

$$\zeta_0 = \frac{-Q(p, \bar{p})}{A(U_f)} \quad (15)$$

$$\zeta_2 = \frac{Q(p, p)}{2i\omega I - A(U_f)}$$

## 2.2 Numerical analysis

The response of the system is calculated through numerical simulation, using a 4<sup>th</sup> order Runge-Kutta method. The flutter speed was determined with an optimisation procedure based on the interval halving method (or bisection method). In the this method, one-half of the current interval of uncertainty is discarded in every stage, until the right solution is found, for the middle point of the final interval (Rao, 2009). From an initial guess for the interval, which is taken based on the flutter speed of the linear system, and with the other parameters fixed, the optimisation procedure seeks to minimise the difference between consecutive peaks of the response in time. If the difference is zero, this gives the condition of self-sustained oscillation. Therefore, the objective function is given by:

$$f(U) = |D_f| - E \quad (16)$$

in which  $D_f$  is the difference between the penultimate amplitude peak and last amplitude peak, and  $E$  is a tolerance. Equation (16) allows the reasoning that in order for flutter to happen, the distance between the peaks must be 0. Since the equations are solved numerically, a tolerance must be considered.

The values of parameters used here are based on values from [16]:  $\beta = 2.5940$ ,  $r_\alpha = 0.5467$ ,  $\gamma = 0.5090$ ,  $\zeta_h = 0.0535$ ,  $\zeta_\alpha = 0.1102$ ,  $x_\alpha = 0.25$ ,  $\rho = 1.2754 \text{ kg/m}^3$ ,  $b = 0.76 \text{ m}$ ,  $\kappa$  varies from  $2 \times 10^{-6}$  to  $8 \times 10^{-6}$  até  $\eta = 3.66 \times 10^{-9}$ ,  $\lambda = 0.48 \times 10^9$ ,  $m = 92.53 \text{ kg}$ ,  $\omega_h = 50 \text{ rad/s}$ . The initial conditions used are  $h = 0.01$ ,  $\alpha = 0.01$ ,  $h' = 0$  e  $\alpha' = 0$  e  $v = 0$ .

### 3 Results

Figure 2 shows amplitude as a function of wind speed, using 4<sup>th</sup> runge kutta method (RK) and multiple scales method (MMS), varying  $\delta$  and fixing  $K = 1$ . Plunge ( $h$ ), pitch ( $\alpha$ ) and voltage( $v$ ) decreases when  $\delta$  increase for this range of wind speed, so cubic nonlinear stiffness reduces LCO amplitudes, for this range. Comparing both methods, we have a good agreement, for plunge, pitch and voltage. The biggest difference between both methods is 10.7%, it is given by voltage for  $\delta = 1$  and  $K = 1$  and  $U = 68$ .

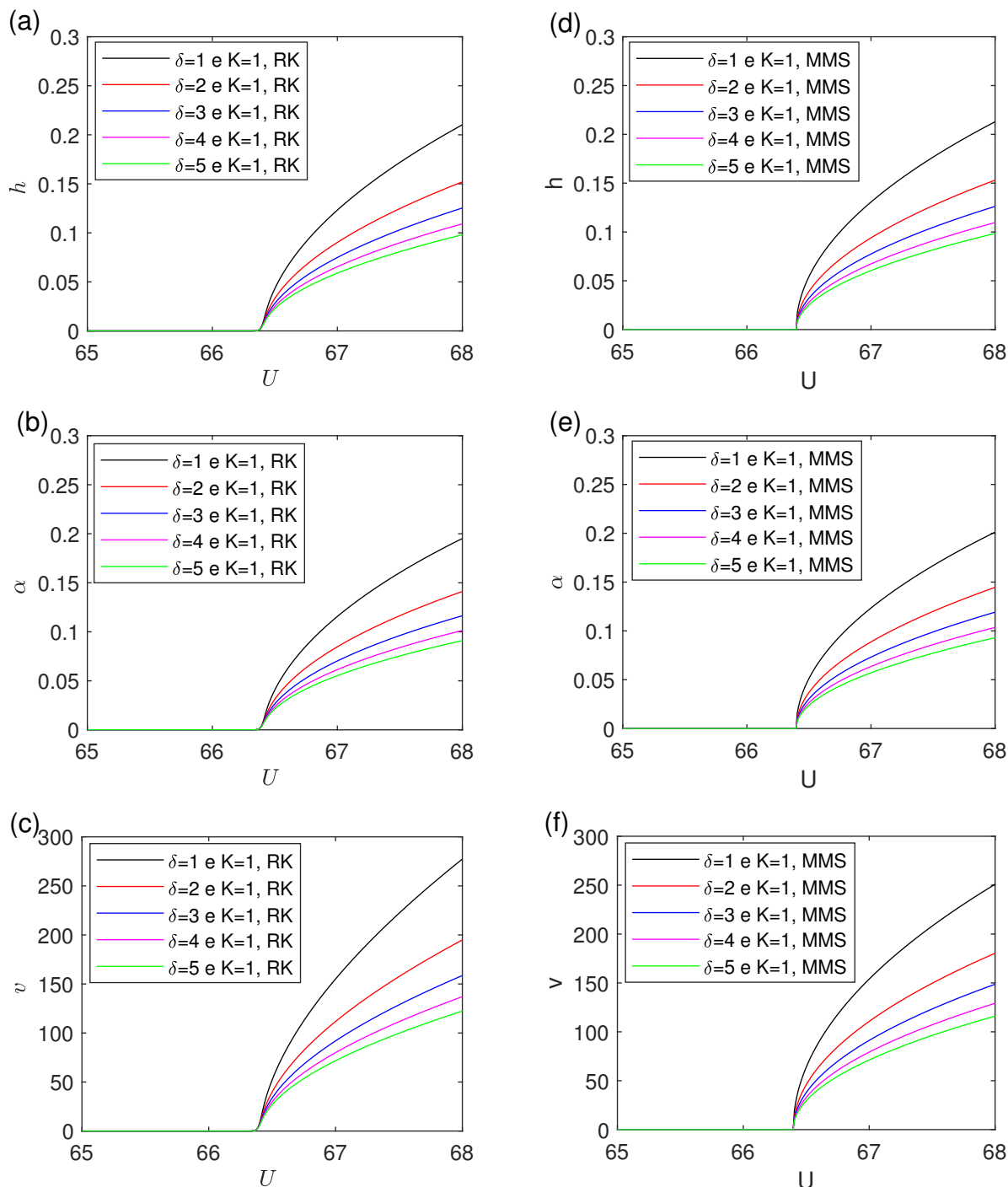


Figure 2. a) Mechanical amplitude (plunge) b) Mechanical amplitude (pitch) c) Electric amplitude as a function of wind speed, 4<sup>th</sup> runge kutta method (RK), d) Mechanical amplitude (plunge) e) Mechanical amplitude (pitch) f) Electrical amplitude as a function of wind speed, using multiple scales method (MMS).

Figure 3 shows amplitude as a function of wind speed, using 4<sup>th</sup> runge kutta method and multiple scales method (MMS), varying  $K$  and fixing  $\delta$ . Plunge ( $h$ ), pitch ( $\alpha$ ) and voltage( $v$ ) decreases when  $K$  increase for this range of wind speed, so quadratic nonlinear piezoelectrical coupling reduces LCO amplitudes, for this range. Comparing both methods, we have a good agreement for plunge and pitch. For voltage it does not present a good approximation, the biggest difference between both methods is 73.9%, for  $\delta = 1$  and  $K = 20$  and  $U = 68$ . It is noticed that we have difference in concavity for voltage from  $K = 10$  between both methods, what explains the difference of values.

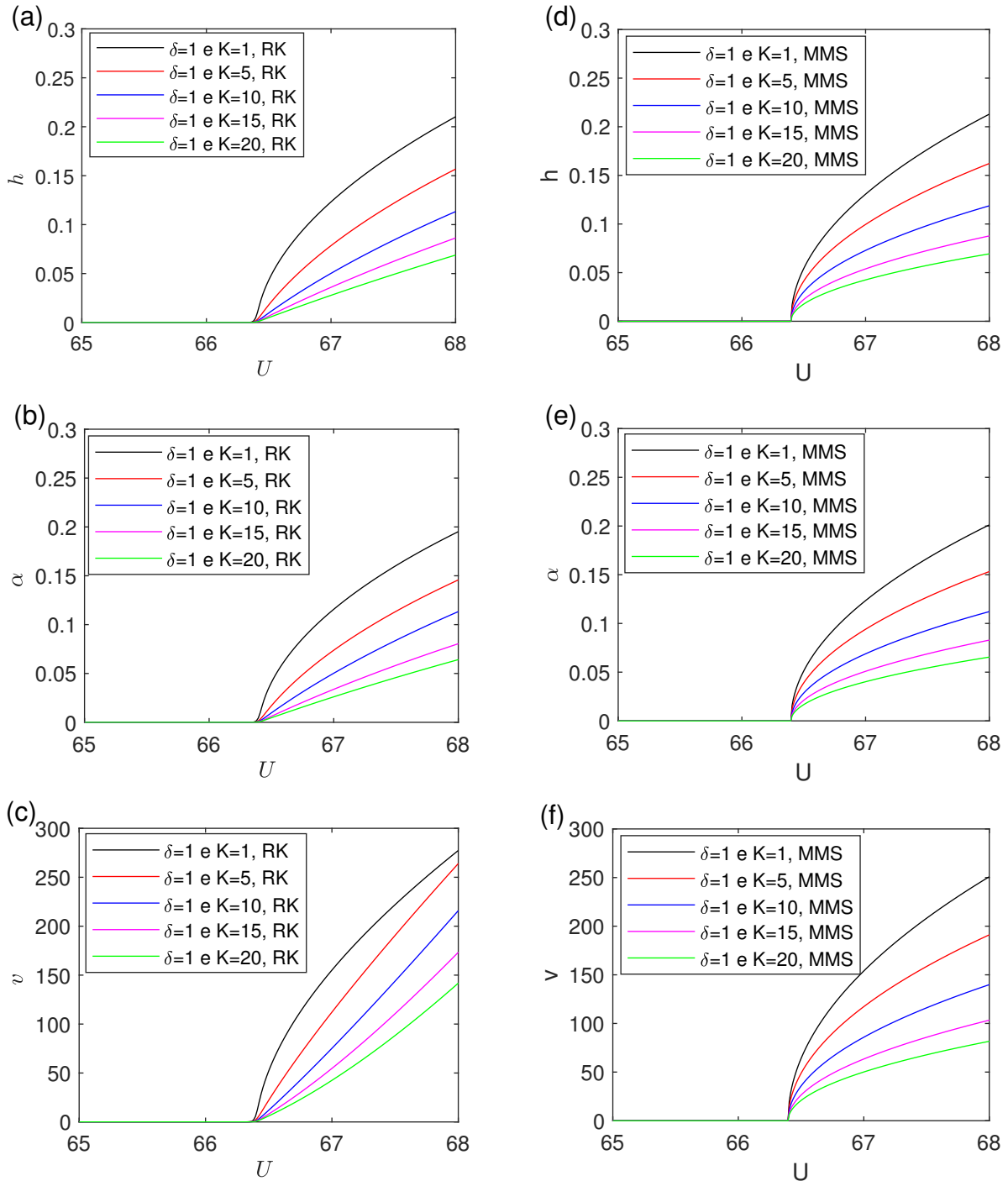


Figure 3. a) Mechanical amplitude (plunge) b) Mechanical amplitude (pitch) c) Electric amplitude as a function of wind speed, 4<sup>th</sup> runge kutta method (RK), d) Mechanical amplitude (plunge) e) Mechanical amplitude (pitch) f) Electrical amplitude as a function of wind speed, using multiple scales method (MMS).

## 4 Conclusions

In this work we explore the method of multiple scales to analyse energy harvesting in aeroelastic system in flutter condition, the approximated solution for the steady state motion of the system with cubic nonlinear stiffness and quadratic nonlinear piezoelectrical coupling was calculated through multiple scales and 4<sup>th</sup> order Runge-Kutta method. The results indicates that amplitude decreases when  $\delta$  and  $K$  increase, so both nonlinearities can reduce LCO amplitudes for wind speed near flutter. Comparing both methods, we have a good approximation, except for voltage, when varying  $K$ . It is important to observe that the results show good agreement in the LCO amplitudes only near the bifurcation.

**Acknowledgements.** The first author thanks CAPES (Coordenação de Aperfeiçoamento de Pessoal de Nível Superior) for the financial support (Process Number 88887.606139/2021-00). The second author thanks CNPQ (grant 309860/2020-2).

**Authorship statement.** The authors hereby confirm that they are the sole liable persons responsible for the authorship of this work, and that all material that has been herein included as part of the present paper is either the property (and authorship) of the authors, or has the permission of the owners to be included here.

## References

- [1] M. Safaei, H. A. Sodano, and S. R. Anton. A review of energy harvesting using piezoelectric materials: state-of-the-art a decade later (2008–2018). *Smart Materials and Structures*, vol. 28, n. 11, pp. 113001, 2019.
- [2] F. I. Petrescu, A. Apicella, R. V. Petrescu, S. Kozaitis, R. Bucinell, R. Aversa, and T. Abu-Lebdeh. Environmental protection through nuclear energy. *American Journal of Applied Sciences*, vol. 13, n. 9, pp. 941–946, 2016.
- [3] A. Bibo and M. F. Daqaq. Energy harvesting under combined aerodynamic and base excitations. *Journal of sound and vibration*, vol. 332, n. 20, pp. 5086–5102, 2013.
- [4] M. G. Kang, W. S. Jung, C. Y. Kang, and S. J. Yoon. Recent progress on pzt based piezoelectric energy harvesting technologies. In *Actuators*, volume 5, pp. 5. Multidisciplinary Digital Publishing Institute, 2016.
- [5] Z. Yang, A. Erturk, and J. Zu. On the efficiency of piezoelectric energy harvesters. *Extreme Mechanics Letters*, vol. 15, pp. 26–37, 2017.
- [6] C. Marqui Jr, D. Tan, and A. Erturk. On the electrode segmentation for piezoelectric energy harvesting from nonlinear limit cycle oscillations in axial flow. *Journal of Fluids and Structures*, vol. 82, pp. 492–504, 2018.
- [7] R. L. Bisplinghoff, H. Ashley, and R. L. Halfman. *Aeroelasticity*, volume 1. Courier Corporation, 2013.
- [8] E. Jonsson, C. Riso, C. A. Lupp, C. E. S. Cesnik, J. Martins, and B. I. Epureanu. Flutter and post-flutter constraints in aircraft design optimization. *Progress in Aerospace Sciences*, vol. 109, pp. 100537, 2019.
- [9] A. Abdelkefi, A. H. Nayfeh, and M. R. Hajj. Modeling and analysis of piezoaeroelastic energy harvesters. *Nonlinear Dynamics*, vol. 67, n. 2, pp. 925–939, 2012.
- [10] A. Triplett and D. D. Quinn. The effect of non-linear piezoelectric coupling on vibration-based energy harvesting. *Journal of Intelligent Material Systems and Structures*, vol. 20, n. 16, pp. 1959–1967, 2009.
- [11] V. C. Sousa, T. M. P. Silva, and C. Marqui Jr. Aeroelastic flutter enhancement by exploiting the combined use of shape memory alloys and nonlinear piezoelectric circuits. *Journal of sound and vibration*, vol. 407, pp. 46–62, 2017.
- [12] A. H. Nayfeh and D. T. Mook. *Nonlinear oscillations*. John Wiley & Sons, 2008.
- [13] H. Liu and X. Gao. Vibration energy harvesting under concurrent base and flow excitations with internal resonance. *Nonlinear Dynamics*, vol. 96, n. 2, pp. 1067–1081, 2019.
- [14] A. Bibo, A. H. Alhadidi, and M. F. Daqaq. Exploiting a nonlinear restoring force to improve the performance of flow energy harvesters. *Journal of applied Physics*, vol. 117, n. 4, pp. 045103, 2015.
- [15] M. Ghommam, A. H. Nayfeh, and M. R. Hajj. Control of limit cycle oscillations of a two-dimensional aeroelastic system. *Mathematical Problems in Engineering*, vol. 2010, 2010.
- [16] C. Marqui Jr and A. Erturk. Electroaeroelastic analysis of airfoil-based wind energy harvesting using piezoelectric transduction and electromagnetic induction. *Journal of Intelligent Material Systems and Structures*, vol. 24, pp. 846–854, 2013.
- [17] E. H. Dowell, H. C. Curtiss, R. H. Scanlan, and F. Sisto. *A modern course in aeroelasticity*, volume 3. Springer, 1989.